Triaging 50 km of dykes

Cesar H. Oboni
Oboni Riskope Associates Inc., Vancouver, B.C, Canada
Franco Oboni
Oboni Riskope Associates Inc., Vancouver, B.C, Canada

ABSTRACT
This paper uses a case history to show how assistance was provided in performing a probabilistic risk breach prioritization of a 50 kilometres long flood-protection dyke of a fluvial-marine area requiring flood and surge protection. Location and details of this job are restricted by confidentiality. Uncertainties and incomplete information were considered in the risk prioritization as detailed engineering analyses and testing were either not available or couldn't be performed due to various issues. The study goal was to show how fast the surface protected by the dykes would flood, in case of one or multiple failures, and estimate the actual capping water depth, i.e. show the influence of topography and tidal pulses on the flooding risks. Potential consequences, thus risks, of flooding strongly depend on water depth and velocity. Crest chainage of the dyke had considerably changed over time due to settlement, reinforcements, construction. The location of low spots was investigated using LIDAR imagery which allowed to build the surface 3-D topographic model. Based on available data an approach was developed to determine the relative failure likelihood of the dyke's "homogeneous" segments. Actual failure locations were forecast in terms of relative probability. The risk register can then evolve and be refined as information is collected, as actions need to be focused on the highest risks structures.

This paper illustrates:
- deployment of the approach using hybrid data sources, such as LIDAR drones and satellites and record, literature;
- results of enhanced risk prioritization techniques.

The deployment brought the following benefits:
- confidence, clear decision-making support;
- clarity, transparency from streamlined risk assessment;
- optimum allocation of mitigative resources and effort, focusing detailed analyses where necessary;
- ease of internal and external communication through using well defined glossary and definitions;
- rational and unbiased lessons learned inclusion.

RÉSUMÉ
Cet article utilise une étude de cas relative à une digue de protection contre les inondations de 50 kilomètres de long dans un estuaire nécessitant une protection contre les inondations et les marées. L'emplacement et les détails de ce cas sont limités par la confidentialité envers le client. Les questions posées demandaient une priorisation probabiliste des possibles brèches dans le but de déterminer les risques. Les incertitudes et les informations incomplètes furent prises en compte dans la hiérarchisation des risques, car les analyses techniques détaillées et les détails géotechniques n'étaient pas disponibles en raison de diverses raisons "historiques". L'objectif de l'étude était de montrer à quelle vitesse la surface protégée par les digues seraient inondées en cas de défaillance de ces dernières, d'estimer la profondeur de l'eau, c'est-à-dire l'influence de la topographie et des marées sur les risques d'inondation. Les conséquences potentielles, et donc les risques, d'inondation dépendent fortement de la profondeur et de la vitesse de l'eau. La crête de la digue avait considérablement changé au fil du temps en raison de tassements, de renforts, de modifications. L'emplacement des points bas fut étudié en utilisant de l'imagerie LIDAR, ce qui permit de construire le modèle topographique 3D de la surface. Sur la base des données disponibles, une approche fut développée pour déterminer la probabilité de rupture relative aux segments "homogènes" de la digue. Les emplacements des possibles défaillances furent prévues en termes de probabilité relative. Le registre des risques peut alors évoluer et être affiné quand de l'information nouvelle est collectée, car les actions de reduction de risques doivent être axées sur les structures à plus haut risque.

Cet article illustre:
• le déploiement de l'approche à l'aide de sources de données hybrides, telles que les drones, LIDAR et les satellites, les archives, et la littérature;
• les résultats des techniques améliorées de hiérarchisation des risques.

Le déploiement a apporté les avantages suivants:
• un soutien clair à la prise de décision;
• la rationalisation et transparence dans l'évaluation des risques;
• l'allocation optimale des ressources et des efforts d'atténuation, en concentrant des analyses détaillées si nécessaire;
• facilité de communication interne et externe grâce à l'utilisation d'un glossaire et de définitions bien définis;

2 INTRODUCTION

This paper describes a probabilistic breach prioritization study bearing on the segments constituting a 50km long river delta dyke and the analysis of one breach location (on a test segment) based on available information (Figure 1). The dyke protects low lying areas from both sea and river flooding.

Detailed engineering analyses and testing were not performed. One specific area was used as a test case for advanced simulations of flooding and simultaneous tidal oscillations.

This paper does not analyze the simultaneous occurrence of a quake and a flood event, or possible damages from prior earthquakes.

The paper shows how fast the low lying areas would flood, in case of a single dyke breach and estimates the actual capping water depth, allowing to understand the influence of topography and tidal pulses, present on most of the layout, on the flooding.

3 AVAILABLE DATA

3.1 Availability of Topographic Data

Topographic LIDAR data was used to conduct the study. Riskope searched historical extant data on floods, tidal oscillations, possible surges and river hydraulic model. The most recent report featured a maximum water level map for the area of interest.
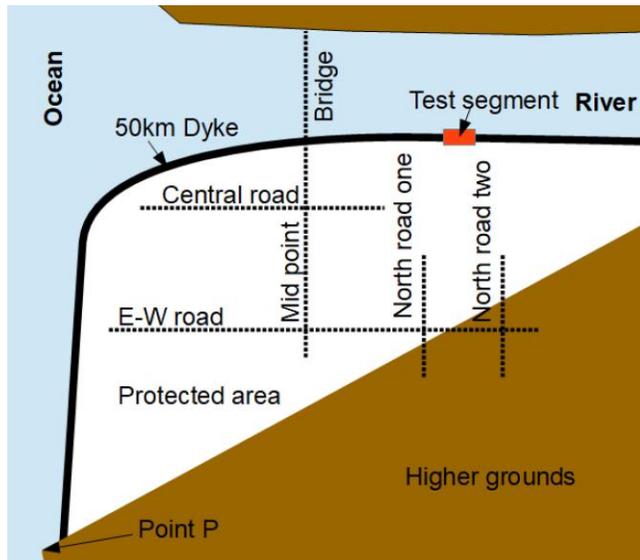

Figure 1 Schematic map of the considered area

The maximum level is not a permanent condition, but a transient one in the areas where the water level is tide-driven. Tides lower the level following their cycle, resulting in water pulsating toward/outward of the protected areas in case of dykes' breaches.

3.2 History of flooding, past failures & hydraulics studies

Various freshets and heavy rainfall events were recorded in the past.

Freshet – The highest freshets occurred in 1894, 1948, and 1972 almost reaching the dyke crest. In each of these instances, no flooding occurred in the protected area. In 1948, however there was minimal local flooding.

Weather Events – the protected area drainage system is reportedly designed to accommodate a 1:10 year storm event. There have been some minor instances of property damage to low-lying properties caused by flooding during heavy rainstorms that exceeded a 1 in 10 year storm event.

4 FREE-BOARD 100YRS ANALYSIS

The value of required free-board usually varies with several dyke's factors including for example: 1. Height, 2. Type of construction material, 3. Top width, etc.

It is generally agreed that the amount of free-board should be increased to protect areas with high value and high loss potential. A review of different free-board requirements in other countries provided some examples of the adopted values (McArthur, 1991).

A survey of crest elevations between 2001 and 2007 indicated that, based on the estimated 100yrs flood elevation, dykes' free-board varied considerably from 0.3m to almost 2m locally. Several areas presented "low spots" when compared to the original 1970 crest design. Thus, previous studies concluded that the levee will not protect against the current 100-year flood event.

Table 1. 100 yrs. flood elevation, dykes' free-board

Parameter	Previous 100yrs flood studies free-board (m)
Minimum	0.3
Maximum	2.15
Average	0.75
Median	0.67
Standard deviation	0.3

5 INTERNATIONAL LITERATURE ON DYKE FAILURES

In the Netherlands there is a database covering 8 centuries and 338 events with an estimated 1735 dyke failures. The table below sets out the main causes of historical dyke failures in the Netherlands.

Storm surges were generally the major cause of dyke failure, followed by high water and ice drift.

Only a small percentage of dykes failed because of external forces. These failures can be attributed to either

humans or animals. Human actions include, for example, dyke piercing, bombing (war or terrorism), ship collision or leaking water pipelines. Many dykes were deliberately breached for strategic reasons, in particular during the 80 Years War (1568-1648) and the Second World War.

Table 2 Mechanism Distribution recorded in the Netherlands for a total of 1735 recorded failures in approximately 11 centuries of dykes history.

Mechanisms	Rate	Comments
Erosion of inner slope protection + crest	67.0%	When overtopped
Ice drift	11.0%	
Erosion or instability of outer slope protection	6.00%	Rip rap, outer slope
Sliding inner slope	5.00%	When overtopped
External (human and animal)	4.00%	Erosion and encroaching
Sliding outer slope	3.00%	Outer slope
Liquefaction of shore line	2.00%	Outer slope
Piping	1.0%	
Micro instability	0.5%	
Horizontal shear	0.5%	
Bursting of inner clay layer	0.0%	
Heave	0.0%	

In the past, storm surges led to major damages, also along the German coastline. Due to climate change it may be expected that the risk of flooding will increase in the coming decades. In order to enhance the knowledge related to extreme storm surges and the assessment of the associated risk, a joint research project named XtremRisK was initiated in the Netherlands. The general aim of the project was to develop methods to quantify the overall flood risk under present and future climate change conditions for an open coast (Island of Sylt, North Sea) and an estuarine setting in an urban area (Hamburg, Germany) using an integrated risk analysis approach (Oumeraci, 2004).

When designing and inspecting dykes, engineers must take into account all the mechanisms that cause dykes to fail. Dutch dyke engineering literature list, for example, thirteen failure mechanisms, among which: 1. Run-over; 2. Wave overflow; 3. Instability of outer slope protection or erosion; 4. Erosion of inner slope protection; etc. (Fig. 2b).

There are more failure mechanisms that can lead to flooding of the protected areas other than overtopping. Another danger is the malfunctioning of dyke crossing structures (e.g. sluices, gates, ship logs; i.e. see Katrina case in US by Kanning et al., 2007; Damrey case in Vietnam by Mai Van et al., 2006a,b).

Only a few case histories of dyke failure due to uplift have been published. It is conceivable that the initiating mechanism has not been recognized in cases of dyke failure caused by uplift, either because of the resulting damage or because of ignorance about this mechanism.

Coastal flood defence structures react differently under the impact of sea loads. The factors that affect structure performance are usually varied. Over recent years, considerable effort has been devoted to improving knowledge related to sea flood defences failures. The appropriate characterization of failure mechanisms of coastal flood defences is a key component in effective reliability analysis and flood risk assessment. Currently, there is an increasing interest to quantify the reliability of coastal flood defences using probabilistic approaches (see the concept, method and application in Bakker & Vrijling 1980; Oumeraci et al., 2001 and Voortman 2002). The probabilistic method allows designers to take into account uncertainties of the input parameters, treat them as the random variables and aims at determination of the true probability of flooding.

The failure mechanisms of a dyke section can be schematized with a fault-tree as in Figure 2.a. These failures of sea dykes can also be presented in relation to their functional elements as in Figure 2.b.
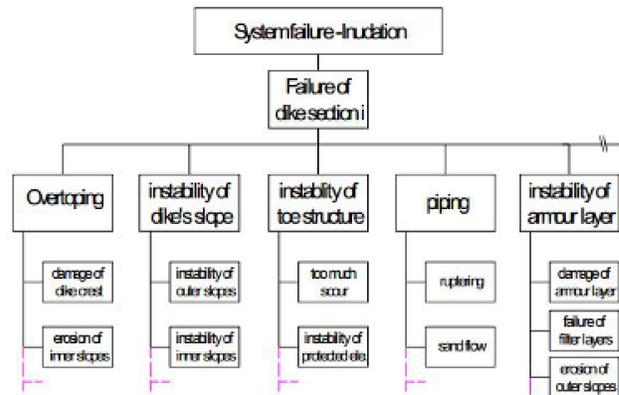

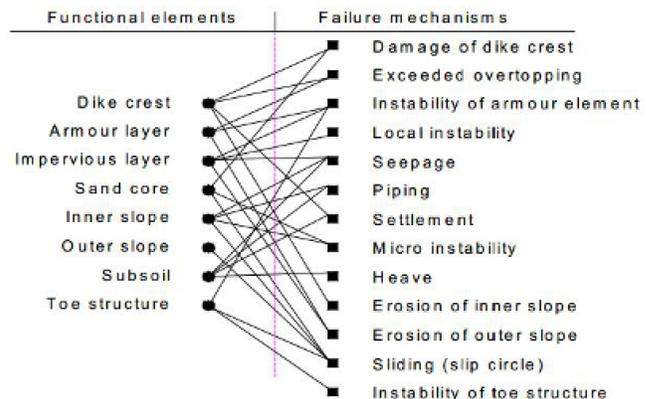Figure 2.a Schematic fault tree of the failure mechanism.

Figure 2.b Failure mechanisms related to dykes functional elements.

The length of a dyke has a considerable influence in the number of expected failures during an event. For example,

with a multiple section dyke system of more than 90km long, the probability of multiple dyke's failures may increase by factor 3 to 10 (Mai Van et al., 2006b) with respect to a shorter system. Most dyke failures are indeed not solitary events. In 58% of the recorded events, the disaster was caused by a series of failures. Major disasters in particular, such as the flood in Zeeland of 1953 and the disaster caused by Hurricane Katrina in New Orleans in 2005, are a combination of a large number of failures. This means that evacuation, flooding and dyke repair analyses, based on a single dyke failure, are only one element of reality and multi-failure simulations should always be carried-out.

6   DYKES BREACH MODELLING

A great deal of data is needed to be able to apply the Netherlands' methods, including information about the sub-soil under the dykes and engineering works. However in our case both those data sets were incomplete or just non-existent. Thus, we proceeded to define an approach to determine the relative likelihood of failure of apparently "homogeneous" segments of the levees. The approach detail is commensurate to available data.

6.1   Dykes failure analysis general procedure

The approach (Section 5.2) is based on a subjective, symptom-driven evaluation of the relative probability of failure calibrated on the Netherlands failure records summary with observable parameters.

A site visit was carried out leading to observations useful in the selection of driving parameters for the probability estimates. The typical earth dyke sections were defined and homogeneous sections amenable to analysis defined.

The actual failure location was predicted based on relative probabilities. Indeed, for each homogeneous sector, the likelihood of failure was estimated. A list of ten "highest hazard (likelihood)" segments prepared.

The next step (Section 5.3) was to evaluate breach characteristics using empirical literature relations based on more than one hundred dam breaches. Initial and "final" breach dimensions were estimated (from 16m up to 200m). At this point the hydraulic modeling (Section 5.4) started with the aim of understanding the development of maximum flooding levels including tidal pulses effects.

6.2   Dyke failure likelihood and prioritization

In the first part of this section we define a way to differentiate cross sections based on observable characteristics which reportedly alter the probability of failure of a dyke. These are listed below:
- Not a low spot
- Riprap present on the "waterside"
- Mild pitch of the dyke on the "dry" side
- Extra dyke width, wide crest width of the embankment
- Finish of the embankment crest (paved, etc.)
- Encroached width, toe erosion, etc.
- Trees on the dyke on the "waterside"

- High visibility (e.g. easily accessible, not private property, close to residences)
- Low stream velocity at the toe of the embankment

The estimated range of the failure likelihoods was split in positive partial contributions by giving relative weights to the positive observable characteristics, based on literature results, as displayed in Table 3.

Table 3. Positive observable characteristics

	Characteristic	Relative Weight
1	Not a low spot	19.30%
2	Riprap on the "waterside"	10.50%
3	Mild pitch of the dyke on the "dry" side	6.60%
4	Extra dyke width, Crest width of the embankment	3.85%
5	Revetment of the embankment crest (paved, etc.)	3.30%
6	Encroached width, toe erosion, etc.	2.75%
7	Tree on the dyke on the "waterside"	1.65%
8	Easily accessible, not private property, close from residences	1.10%
9	Low velocity at the toe of the embankment	0.55%

This lead to determining the segments' breach likelihood and finally to the prioritization for each segment breach probability based on positive observable characteristics (extant mitigative measures and features) as shown in Figure 3.
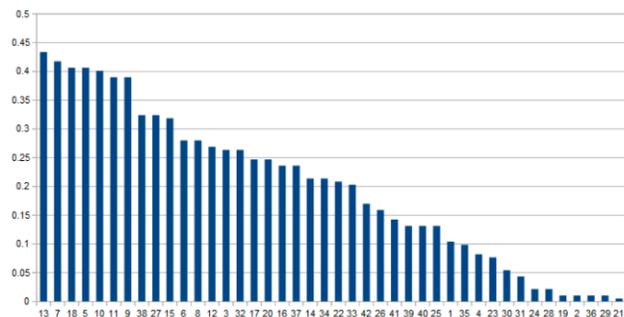

Figure 3 Breach likelyhood (vertical axis) based on observable characteristics for the 41 segments.

6.3   Breach Width Estimation

One important step in dykes' breach modeling is the prediction of the incoming flow which of course depends on the size of the breach(es). Efforts have been made in developing models that accurately predict breach characteristics, but many uncertainties still exist (Franca, & Almeida, 2004; Morris, 2005; Zagonjolli, & Mynett, 2005).

Due to the incomplete understanding of breach formation process and the limited capabilities of mathematical description of dam breaching mechanisms, available models rely on many assumptions. The U.S. Bureau of Reclamation (U.S. Bureau of Reclamation, 1988) suggested that for earth fill dams the ultimate width of a rectangular dam breach shape equals three times the initial water depth in the reservoir measured to the breach bottom elevation assumed to be at the stream bed elevation.

Of course, such a statement should be modified for dykes, before it could be used, in absence of any other information. This relationship was used as a guideline in the National Weather Service Simplified Dam Break Model (Fread, and Lewis, 1998). Hagen (1982) analyzed 18 historical events of dam failures due to overtopping. MacDonald and Langridge-Monopolis (1984) analyzed 42 dams: 30 earthfill and 12 non–earthfill dam breaches (rockfill and other dams with protective concrete surface layers or core walls). The height of the dams varied from 6 to 93m.

Singh and Snorrason (1982; 1984) analyzed some historical earth-fill dam failure events due to overtopping. One finding of this analysis was the identification of a strong correlation between breach width and dam height. US Army Corps of Engineers HEC-1 and National Weather Service BREACH (Fread, 1988) models are usually used for predicting the peak outflow. Costa (1985) analyzed 31 historical dam failure events. The heights of the dams considered in the analysis varied from 1.8m to 83.8m, while the volume of the reservoir at the failure time ranged from 3.8×10^3 m^3 to 7.0×10^8 m^3. No distinction was made between different failure modes and dam types.

There is no significant difference between the regression equations obtained by Mac-Donald and Langridge-Monopolis (1984) and Costa (1985), though the first authors included only earthfill dams in the analysis, the second author considered both earthfill and non–earthfill dams. Froehlich (1987) analyzed 22 embankment dam failures with height of water ranging from 3.4m to 77.4m and volume of water ranging from 0.1 to 310 million m^3. Wahl (2004) carried out an uncertainty analysis of the empirical equations using a compiled database of 108 dam failure events. In the analyses no distinction was made between different failure modes (the same stands for Costa, 1985) although it is clear that for peak outflow prediction based on dam height and reservoir storage, the failure mode is important. In a 2013 study by Nourani & Mousavi (2013), 142 embankment dam breach data were collected from reliable references and dam breach equations analyzed. Dimensional analysis and multiple regression were used to predict maximum outflow from an earth dam breach. Uncertainty of empirical relations was determined using an appropriate statistical method. Based on a comparison between methods, the Nourani & Mousavi approach was considered for this study.

The following general results were derived by Nourani & Mousavi (2013) from collected data by studying 142 embankment dam breaches:

$2*h_d<=B_m<=3*h_d$ where   [1]
B_m=average breach width (m); h_d = dam height (m)

B_{top}/B_{bottom}= 1.13-1.64 width at top, bottom of the breach.

If we note as V_w the water volume above break point of bottom (m^3), which in the case of a flood spanning over several weeks can be considered "infinite" and h_b the height of water above breach bottom the analyses performed in the study yielded the following regression:

B_m= 2.2839* $V_w^{0.0635}$ * $h_b^{0.8481}$ with r=0.918
    [2]

Using the formula [1] we evaluated an initial breach width of 16m assuming water elevation interpolated from extant reports, breach bottom elevation at +0.5m above toe and an "infinite" water volume. Elevation +0.5m corresponds to the bottom of the breach, with eroded volume equal to zero, because at that level there is no water movement through the breach.

Some authors (Schippa, Pavan 2006) suggested breach width evolution analyses based on the evaluation of solids transportation. Such a method (Smart, 1984, Smart & Jaeggy, 1983) was implemented considering the erosional capacity of the incoming/outgoing waters on the two exposed faces of the dyke's breach. It was assumed that the bottom of the breach would be "stable" and located at 0.5m elevation.

A grain size curve was assumed for the dyke, based on experience.

The analysis yielded the graph of Fig. 4 with the water elevation in abscissa and eroded volume in m^3/s in the vertical axis.

It can be concluded that for the highest water levels, the dyke loses approx. 30 l/s (0.03m^3/s) or roughly 2 m^3/min per breach face. Thus, a dyke with a section of 40 m^2 (similar to the profile we can infer from topographic data) would widen by approx. 3m/hr.

Thus, assuming that a tide "pulse" lasts 2-3 hours, the breach could have widened by 12m to 20m. Thus, it can be inferred that the initial 16m breach would possibly evolve, if undetected and not mitigated to 28m-36m after one tide cycle, more in later cycles. For example, in the test segment we are inclined to believe that the breach could establish with a final width of approx. 60m.

Of course, the widening will not last indefinitely, because morphological limits (less erodible features) will most likely occur. In Phase I we considered 100m and then 200m wide fully developed breaches, in an effort to carry out a "safe-side" parametric influence study.

6.4   Hydraulic model for potential Interior flood depths

The purpose of this analysis was to evaluate the water depths as a function of time in case of a breach of a "test" segment (See Fig. 1). As mentioned above, tidal oscillations were included in the analyses. Tidal effects are reportedly significant up to the mid point of the system. Like in extant reports "winter condition" tide and a two month (seven weeks) long flooding event were considered. Tidal oscillations models were prepared based on data from available reports. The oscillation (and of course, the resulting water elevation) determines the inflow rates. After calibration, the model included the outflow computation during tide recession. The simulation time was set from

breach time to over 12 days in order to allow the analysis of a variety of transitory water level conditions.
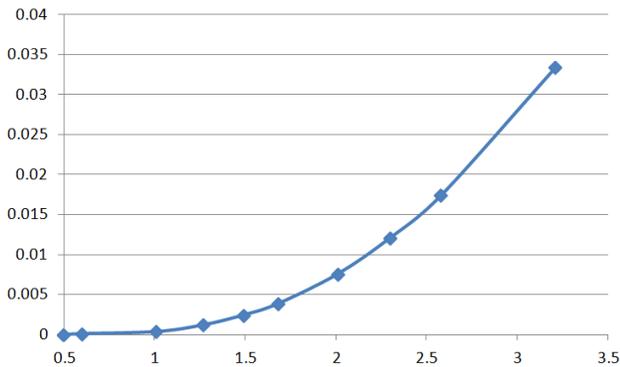

Fig. 4 Eroded volume in m^3/s on the y-axis vs. water elevation on the x-axis.

A critical point for this type of simulation is and remains the availability of accurate topography, including local anomalies, internal barriers (road fills), walls, buildings and ditches, etc. The available LIDAR topographic model obtained for free for this study has 50cm contour lines and channels and ditches were added manually after Google Earth observation of the flat area. The minimal altitude of Mid-point Bridge Street, which acts as a defence for the western residential neighborhoods of the protected area in case of the test segment breach, was set at elevation 1.5 m. In contrast, Bridge street represents a preferential water course during flooding. Main ditches such as the one along North Road Two all the way to Central Road and other transverse channels, which are considered to be of significant influence for the inflow/outflow were also included. Finally, the simulation included specific assumptions to give due consideration to residential density and the numerous industrial buildings in the strip of land between North Road One and Mid-point Bridge Street.

For this study a harmonic function [3] was adopted to model winter tides as follows (Vultaggio, 1980):

$$H(t)= K0+ O1 \quad cos[\omega(O1)t+\varphi(O1)]+K1 \quad cos[\omega(K1)t+\varphi(K1)]+..+ MS4 \; cos[\omega\,(MS4)t+\varphi(MS4)] \qquad [3]$$

Where H(t) is the water level at time t, constants O1, K1, M2, S2, N2, K2, P1, M4, MS4 are the "height constituent", ω are the angular velocities function of the period of the oscillating movement and φ is the phase of the oscillating movement. All of the above are functions of the location, latitude, time, etc. Triton (2006) reported all the tide harmonics and related phases.

To develop an acceptable simulation, we selected the first 9 most important tidal height constituent O1, K1, M2, S2, N2, K2, P1, M4, MS4 and the correct associated phases, function of the analyses at Point P.

This function [3] represents the astronomic tide (without climatology effects).

From extant reports and the historic series at Point P it can be inferred that the two worst months for surge events are December and January. These are also the months where the likelihood of a flooding is very low. Nevertheless, the scenario combination leads to a Winter Condition, which is the worst-case scenario.

One of the goals of the analysis was to determine which variables have the strongest influence in the determination of the flooding depth inside the protected area.

The simulations showed that the assumption of the initial breach development time (assumed to be 5hrs) is negligible at event scale. However, the breach widening and simultaneous tide pulse determine a progressive filling of the protected area theoretical reservoir as depicted in Figure 5.
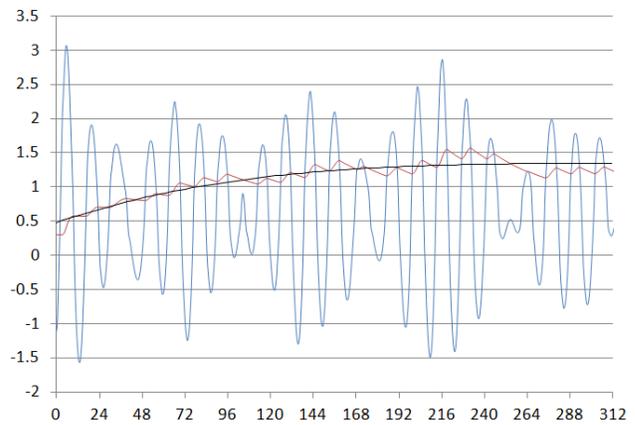

Figure 5 Progressive raise of flood water (red at breach, black 500m from breach) during the development of a 16m breach of the Test segment, under tidal oscillation (blue).

Figure 5 shows that for a 16m breach (stable width), the flooding level stabilizes after 8-10 days around 1.5 m (internal average level 1.21 m). This means that high tides "push" water inside the protected area, under the assumptions made to this point, but water also outflows during low tides, finally reaching an equilibrium. The interior water level follows, with delay, the outside levels.

These first results showed it would be interesting to test the effect of a wider (fully developed) breach, for example 100m and 200m wide. Figure 6 and 7 display the respective results.

With the widening of the final breach the delays are reduced. Maximum water depth peaks increase, but the "average" flooding depth does not change significantly with respect to the 16m breach. As stated earlier, these analyses do not consider any mitigative intervention during the event or topographic details inside the protected area.

The simulation shows a first phase (12hrs from breach) with a significant pulse, in correspondence to the first tidal peak, which floods approximately 9.6km². That corresponds to 72% of the area flooded after 160hrs (13.2 km²), or 54% of the area flooded after 300hrs (17.7 km²).

The area that floods faster is also the area with the highest waters. Flooding progresses by steps dictated by successive tidal peaks. In particular, there are significant flooding progressions after 70-140-220 hrs. due to tidal peaks. These values are interesting for the preparation of mitigative/ protection/ emergency activities deployment plans.

In summary, it was possible to evaluate that the flooded area, even after considerable time, will be exposed to better conditions than described in prior reports, due to the inflow/outflow effects linked to tidal oscillations. Of course, the situation would progressively worsen if several breaches would occur and no emergency protection/actions were undertaken.
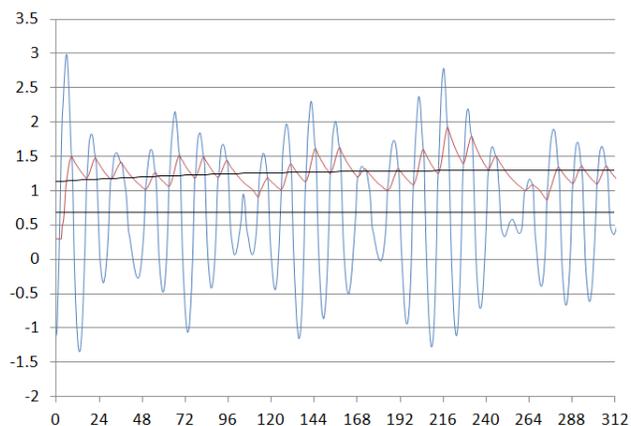

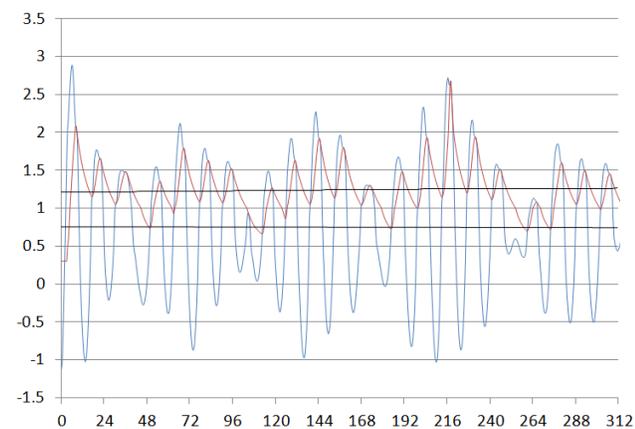Figure 6 Same graph as in Figure 5, but with 100m wide breach

Figure 7 Same graph as in Figure 6, but with 200 m wide breach

It can be concluded that the widening of one breach or the existence of various breaches leads to higher internal levels, with less delay with respect to tidal pulses.

The elevation of the bottom of the breach was also evaluated (standard case 0.5m, alternative 0m), but it was

concluded that this variable had little impact on the final results.

Finally, the theoretical storage volume of the protected area "reservoir" was reduced to get a first idea of the impact of topographic partitioning of the volume (for example, low-spots, drainage ditches, road fills. It became immediately apparent that, as expected, the presence of these topographic "anomalies" has very significant repercussions on water levels value, time to establish and location.

In general terms it was evaluated, based on the assumptions and with the topography/data available to date, that even with a 90m long breach in the test segment, at 1km distance, water depth will be in the order of 1m, whereas at 3km, in general, depths will be lower (of course these are "averaged" estimates, as local depressions will have higher waters. Those values are to be compared with the water levels at breach location, depicted in Figure 8.
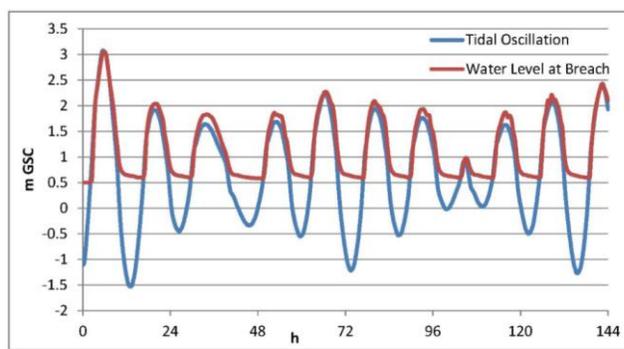

Fig. 8 Water level at breach (y-axis) vs. time in hour (x-axis) after breach

Ultimately, it was estimated that the test segment breach would develop flooding on the West side between North Road One and Mid Point and Bridge Street with possible overflows of both in local depressions. In the East side flooding would invade the fields and agricultural areas. In the South, the East-West road constitutes a barrier that would ultimately be bypassed via extant underpasses.

The East-West road behaves as a sort of internal dyke which will prevent, up to a certain point, the waters from flowing towards the South. However, at the North Road One crossing the underpass will allow flow in the Southern direction.

Armed with water levels, water velocity it was finally possible to define the consequences of the breach both in terms of potential harm to residents and to the existing structures and infrastructures, allowing for a complete risk analysis.

7   CONCUSIONS

This study showed that it is possible to integrate highly uncertain data on existing structures with detailed topography, space observation, hydrological and ocean data to complete a quantitative risk assessment of a dyke system.

Key to sustainable results is the triaging of the dykes, i.e. the probabilistic evaluation of their proneness to fail.

In this particular case it was concluded that the widening of one breach or the existence of various breaches lead to higher internal levels, with less delay with respect to tidal pulses. The elevation of the bottom of the breach had little impact on the final results.

As expected the presence of topographic "anomalies" has very significant repercussions on water levels value, time to establish, and location.

The triaging and risk assessment allowed to guide rational and sustainable emergency procedures, preparedness and evacuation plans.

8 REFERENCES

Bakker, W.T; Vrijling J.K (1980). Probabilistic design of sea defences. Proceedings International Conference on Coastal Engineering 1980.

Costa, J. E. (1985) Floods from dam failures, Open-file report, U.S. Department of the Interior Geological Survey, Denver, USA.

Franca, M. J. and Almeida, A. B. (2004) A computational model of rockfill dam breaching caused by overtopping (RoDaB), Journal of Hydraulic Research 42(2), 197–206.

Fread, D.L. (1988) (revised 1991) BREACH: An Erosion Model for Earthen Dam Failures, National Weather Service, National Oceanic and Atmospheric Administration, Silver Spring, Maryland.

Fread, D.L. and Lewis, J.M. (1998) NWS FLDW A V Model: The Replacement of DAMBRK for Dam-Break Flood Prediction. Hydrologic Research Laboratory, National Weather Service (NWS), NOAA Silver Spring, Maryland 20910.

Froehlich, D. C. (1987) Embankment-dam breach parameters, Proc. of the ASCE National Conference on Hydraulic Engineering, Williamsburg, Virginia, USA, 570–575.

Hagen, V. K. (1982) Re-evaluation of design floods and dam safety, Proc. of 14th Congress of International Commission on Large Dams, Rio de Janeiro, Brasil, 475–491.

Kanning, W., van Baars, S., van Gelder, P.H.A.J.M., & Vrijling, J.K., (2007). Lessons from New Orleans for the design and maintenance of flood defence systems. Submitted paper for Research, Codes and Specification, no. 141, Gouda, The Netherlands.

MacDonald, T. C. and Langridge-Monopolis, J. (1984) Breaching characteristics of dam failures, Journal of Hydraulic Engineering, 110(5), 567–586.

Mai Van, C., van Gelder, P.H.A.J.M., & Vrijling, J.K., (2006a). Safety of coastal defences and flood risk analysis. European Safety and Reliability (ESREL), Safety and Reliability for Managing Risk, ISBN 13: 978-0-415-41620-7, Taylor & Francis/Balkema, Leiden, The Netherlands, Vol. 2. ESREL2007, Stevanger June 2007, Norway.

Mai Van, C., van Gelder, P.H.A.J.M., & Vrijling, J.K., (2006b). Foreshore erosion and scour induced failure of sea dikes. Proceedings Third international conferences on Scour and Erosion, ICSE 2006 November 1-3, 2006 Amsterdam, CURNET, ISBN-10 90-376-0503-6/ ISBN-13 978-90-376- 0503-7. The Netherlands.

Morris, M. W. (2005) IMPACT: Final technical report, Proc. of the 1st IMPACT Workshop, HR Wallingford, UK.

Nourani, V. and Mousavi, S. (2013) Evaluation of Earthen Dam-Breach Parameters and Resulting Flood Routing Case Study: Aidoghmosh Dam, International Journal of Agriculture Innovations and Research, Volume 1, Issue 4, ISSN (Online) 2319-1473.

Oumeraci, H. (2004), Sustainable coastal flood defences: scientific and modelling challenges towards an integrated risk-based design concept. Proc. First IMA International Conference on Flood Risk Assessment, IMA - Institute of Mathematics and its Applications, Session 1, Bath, UK, pp. 9-24.

Oumeraci, H., Allsop, N.W.H., Groot, M.B. de, Crouch, R., Vrijling, J.K., Kortenhaus, A., Voortman, H.G., (2001). Probabilistic design tools for vertical breakwaters. Balkema, Rotterdam, 2001.

Schippa, L., Pavan, S., Modello fisicamente basato per la formazione di brecce negli sbarramenti in terra, xxx° Convegno di idraulica e costruzioni idrauliche - idra 2006

Singh, K. P. and Snorrason, A. (1982) Sensitivity of outflow peaks and flood stages to the selection of dam breach parameters and simulation models, Technical Report 289, State Water Survey Division at the University of Illinois, USA.

Singh, K. P. and Snorrason, A. (1984) Sensitivity of outflow peaks and flood stages to the selection of dam breach parameters and simulation models, Journal of Hydrology, 68, 295–310.

Smart, G.M., Sediment transport formula for steep channels. Journal of Hydraulic Engineering, (1984), 110(3), pp. 267-276.

Smart, G. M., Jaeggi, M.N.R., Sediment Transport on Steep Slopes. Mitt.,Versuchsanstalt für Wasserbau Hydrologie und Glaziologie, ETH-Zürich, 64. 191 pp.,1983

U.S. Bureau of Reclamation (1988) Downstream hazard classification guidelines, ACER Technical Memorandum No. 11, Assistant Commissioner-Engineering and Research, U.S. Department of the Interior, Denver, Colorado.

Voortman, H.G. (2002), Risk-based design of large-scale flood defence systems. Phd-thesis, Delft. Series on ocean engineering, Volume 17, World Scientific, 2002

Vultaggio, M., Maree e correnti di marea, Dispense Navigazione 2 vol. 1 Capitolo 8, Università degli studi di Napoli "Parthenope", Sezione di Navigazione del Dipartimento di Scienze Applicate, 1980.

Wahl, T. L. (2004) Uncertainty of Predictions of Embankment Dam Breach Parameters, Journal of Hydraulic Engineering, 130(5), 389-397.

Zagonjolli, M. and Mynett, A. E. (2005) Dam breach analysis: A comparison between physical, empirical and data mining models, Proc. of the 29th IAHR Congress Seoul, South Korea, 753-75